Current Research in Food Science 5 (2022) 96–101

Contents lists available at ScienceDirect

Current Research in Food Science

journal homepage: www.sciencedirect.com/journal/current-research-in-food-science

Short Communication

# Improving the mechanical properties and thermal stability of sodium alginate/hydrolyzed collagen films through the incorporation of $SiO_2$

Luís Marangoni Júnior [a,*], Plínio Ribeiro Rodrigues [b], Renan Garcia da Silva [a,b], Roniérik Pioli Vieira [b], Rosa Maria Vercelino Alves [a]

[a] Packaging Technology Center, Institute of Food Technology, Campinas, São Paulo, Brazil
[b] Department of Bioprocess and Materials Engineering, School of Chemical Engineering, University of Campinas, Campinas, São Paulo, Brazil

ARTICLE INFO

*Keywords:*
Biopolymer
Sustainable film
Mechanical properties
Food packaging.

ABSTRACT

Biopolymer-based films have become leading alternatives to traditional fossil-based packaging plastics. Among the countless types of biopolymers with potential for such applications, films containing hydrolyzed collagen in their composition were scarcely explored. This study determined the effect of different loads of nano-$SiO_2$ (0, 2, 6, 8 and 10% w/w of sodium alginate) in the sodium alginate (SA) and hydrolyzed collagen (HC) blend films in terms of structure, thickness, mechanical properties, and thermal stability. The results indicated an improvement in the general mechanical and thermal behavior. Tensile strength increased from 18.2 MPa (control sample) to 25.4 MPa for the SA/HC film incorporated with 10% nano-$SiO_2$. In the same condition, the film's elongation at break improved impressively (from 19.5 to 35.8%). Thermal stability improved slightly for all proportions of nano-$SiO_2$. Therefore, the addition of nano-$SiO_2$ can be an easy and simple strategy to improve crucial properties of SA/HC blend films, increasing its performance for future application as sustainable packaging.

## 1. Introduction

Synthetic plastic materials are widely employed in food packaging applications for their excellent properties (Marangoni et al., 2020). Although these polymers offer many advantages, such as protecting food from external conditions, the accumulation of these materials due to incorrect disposal remains a serious environmental problem (Moreira Gonçalves, Gomes Motta, Ribeiro-Santos, Hidalgo Chávez and Ramos de Melo, 2020). The development and application of packaging using raw materials from renewable sources is growing, since the play a fundamental role in reducing negative impacts on the environment. The most used renewable source polymer for film and coating manufacture are composed polysaccharides and proteins (Vianna et al., 2021).

Polysaccharides represent an attractive alternative for the production of films since they are abundant, inexpensive, and biodegradable (Nesic et al., 2020). Sodium alginate (SA) is a promising biomaterial with good film-forming properties for applications such as food packaging (Mousavi et al., 2021), and in the medical field (Abou-Okeil et al., 2018; Gheorghita Puscaselu, Lobiuc, Dimian and Covasa, 2020). SA is a natural anionic polysaccharide that is a by-product of the extraction of iodine and mannitol from brown algae. Its molecule is composed of β-d-manuronic acid (M) and α-l-guluronic acid (G) linked by a bond (1 → 4) (Kloster et al., 2017). SA contains abundant functional groups, such as hydroxyl and carboxyl, which can be easily modified to other functional groups (Zhang, Xu and Yang, 2021), and can help blending with other biopolymers, such as proteins, for obtaining better properties (Castiello et al., 2009).

Hydrolyzed collagen (HC) is a low-cost by-product protein from the tanning industry, and can be used in a mixture with SA, given the notable adhesive properties of proteins and their good processability (Marangoni Júnior, Rodrigues, da Silva, Vieira and Alves, 2021a; Seggiani et al., 2019). HC is a polypeptide compound made by additional hydrolysis of denatured collagen, with lower molar mass (3–6 kDa) than that of native collagen (285–300 kDa), low viscosity and better solubility in water (Denis et al., 2008; Zhang, Sun, Li, Liu and Su, 2006). Hence, incorporating HC in other bio-based films can be an easy strategy to take advantage of its properties and expand the use of this abundant raw material, often resulting in biodegradable (potentially even edible) packaging materials (Pei et al., 2013).

One of the most interesting biopolymer formulation strategies is adding nano-reinforcements, since they can alter the hydrophilic nature of polysaccharide/protein films and provide better mechanical

* Corresponding author. Av. Brasil, 2880, CEP: 13070-178, Campinas, SP, Brazil.
*E-mail address:* marangoni.junior@hotmail.com (L. Marangoni Júnior).

https://doi.org/10.1016/j.crfs.2021.12.012
Received 3 October 2021; Received in revised form 17 December 2021; Accepted 22 December 2021
Available online 29 December 2021

properties (Condés et al., 2018). Nano-$SiO_2$ is an amorphous white powder with a three-dimensional structure (Tian et al., 2020), forming non-toxic, stable, and durable multifunctional inorganic particles (Zhu et al., 2021). The distinctive characteristics of nano-$SiO_2$, including small size, large specific surface area, high surface energy, unsaturated chemical bonds, and presence of hydroxyl group on the surface result in easy dispersion of nano-$SiO_2$ throughout the polymeric matrix (Tabatabaei et al., 2018).

Our group recently investigated concentration and dispersion thresholds of nano-$SiO_2$ in pure sodium alginate composite films. We showed that good dispersions are obtained at nano-$SiO_2$ concentrations lower than 1.5%, but saw no impact on mechanical properties (Júnior, da Silva, Anjos, Vieira and Alves, 2021). Therefore, this research aims to develop sodium alginate/hydrolyzed collagen films with different concentrations of nano-$SiO_2$ (2–10% w/w of SA) to improve the properties. An investigation of the impact of nano-reinforcement on the physicochemical and morphological properties of the films is provided.

## 2. Material and methods

### 2.1. Materials

Sodium alginate (SA) and glycerol (Dinâmica Química Contemporânea Ltda, Indaiatuba/SP, Brazil), hydrolyzed collagen (HC) (NaturalLife, São José do Rio Preto/SP, Brazil), nano-$SiO_2$ ($SiO_2$), Aerosil® 200, with average particle size of 12 nm, and BET surface area of 200 $m^2/g$ (Evonik/Degussa Ltda, Americana/SP, Brazil) (Guha, 2010), were used as received.

### 2.2. Preparation of the films

The SA/HC/$SiO_2$ composite films were prepared based on our previous work that aimed to evaluate the interactions of the material with water (Marangoni Júnior, Silva, Vieira and Alves, 2021b). In summary, sodium alginate solutions (4% w/w) were prepared by dissolving the biopolymer in distilled water containing glycerol as a plasticizer (30 g/100 g of sodium alginate), hydrolyzed collagen (10 g/100 g of SA), and different added concentrations of $SiO_2$ nanoparticles (0, 2, 6, 8 and 10 g/100 g of SA). Film-forming solutions were heated to 80 °C with stirring for 20 min. Subsequently, the final solutions were treated in an ultrasound bath for 15 min, to ensure homogeneity and elimination of bubbles. After this step, 50 g of film-forming solutions were poured into polystyrene Petri dishes (diameter 14 cm) and dried at 40 °C for 24 h in a forced air circulation oven. Finally, after removing the films from the plates, all the samples were stored in an air-conditioning chamber (Weiss Technik, Reiskirchen, Germany) at 25 °C and 75% relative humidity (RH), prior to the characterization processes. Table 1 describes the composition and nomenclature of the different film samples.

### 2.3. Characterization of films

#### 2.3.1. Film morphology

Images of surface (magnification of 1000 × ) and cross section (magnification of 2500 × ) of the composite films were obtained using scanning electron microscopy (SEM) (Leo 440i, LEO Electron Microscopy/Oxford, Cambridge, England). The samples were previously fractured with liquid nitrogen, then fixed in metallic support with the aid of double-sided carbon tape and covered with gold in a sputter coater (SC7620, VG Microtech, Kent, United Kingdom). The visualization was performed with a voltage of 15 kV and a current of 50 pA.

**Table 1**
SA/HC/$SiO_2$ film-forming solutions compositions (%).

| Materials | SA/HC | SA/HC/2%$SiO_2$ | SA/HC/6%$SiO_2$ | SA/HC/8%$SiO_2$ | SA/HC/10%$SiO_2$ |
|---|---|---|---|---|---|
| **Sodium alginate (SA)** | 4.00 | 4.00 | 4.00 | 4.00 | 4.00 |
| **Hydrolyzed collagen (HC)** | 0.40 | 0.40 | 0.40 | 0.40 | 0.40 |
| **Glycerol** | 1.20 | 1.20 | 1.20 | 1.20 | 1.20 |
| $SiO_2$ | – | 0.08 | 0.24 | 0.32 | 0.40 |
| **Water** | 94.40 | 94.32 | 94.16 | 94.08 | 94.00 |

#### 2.3.2. Fourier-transform infrared spectroscopy (FT-IR)

FT-IR analysis were recorded using a Thermo Scientific spectrometer (Nicolet Continuum, Madison, USA). For all composite films, it was used the attenuated total reflectance mode, ATR (Germanium crystal), employing the software Smart Omni Sampler, at 4000-650 $cm^{-1}$, with a resolution of 4 $cm^{-1}$, scan: 32–64. The measurements of each sample were performed for the same sample mass and strictly maintaining the same analysis conditions.

#### 2.3.3. Thermogravimetric analysis (TGA)

Thermal stability testing was performed using a Mettler Toledo Thermogravimetric Analyzer (TGA), model TGA/DSC1 (Schwerzenbach, Switzerland). Measurements were performed in film samples of 10 mg heated from 25 to 600 °C, in a nitrogen flow of 50 mL $min^{-1}$, at a heating rate of 20 °C $min^{-1}$.

#### 2.3.4. X-ray diffraction (XRD)

X-ray diffraction was recorded on an X-ray analyzer (X'Pert-MPD, Philips, Almelo, Netherlands). The XRD measurements of composite films were operated with Cu Kα radiation (λ = 1.54056 Å) at a scan rate of 0.033333°/s (step = 0.04° and time per step = 1.2 s), with the accelerated voltage of 40 kV and the applied current of 40 mA, varying from 5 to 60°.

#### 2.3.5. Film thickness

The thicknesses of the composite films were determined at five random points from five specimens per formulation sample using a system composed of a flat granite base and comparator clock (Mitutoyo Co., Kawasaki-Shi, Japan), with 0.1 μm resolution (ISO-4593, 1993).

#### 2.3.6. Mechanical properties

The samples were cut with a 15 mm width in high precision equipment (RDS-100-C, ChemInstruments, OH, USA). Then, they were conditioned, for 48 h, at 25 ± 2 °C and 75 ± 5% RH. Tensile strength (MPa), elongation at break (%) and modulus of elasticity (MPa) were determined following a standard method ASTM-D882 (2018), using a universal testing machine (Instron, 5966-E2, Norwood, USA), with a 100 N load cell, speed of 12 mm $min^{-1}$ and with initial grip separation of 50 mm. Each film formulation was tested at least 4 replicated and their average reported.

#### 2.3.7. Statistical analysis

The results were statistically evaluated by analysis of variance (ANOVA). Comparisons among mean values were determined by Tukey's tests ($p < 0.05$). The results were expressed as the mean ± standard deviation.

## 3. Results and discussions

### 3.1. Film morphology

Fig. 1 (a) and (b) show the surface and cross-section of the control films. Although the films apparently presented a uniform and smooth surface, a more accurate evaluation in the cross section indicates the occurrence of numerous micrometric-sized pores that may indicate low compatibility between alginate and hydrolyzed collagen. A slight surface roughness (Fig. 1 (c)) appears with the addition of 2% nano-$SiO_2$, but Fig. 1 (d) shows a relatively appropriate dispersion throughout the polymer matrix in the cross-section image. However, small domains of

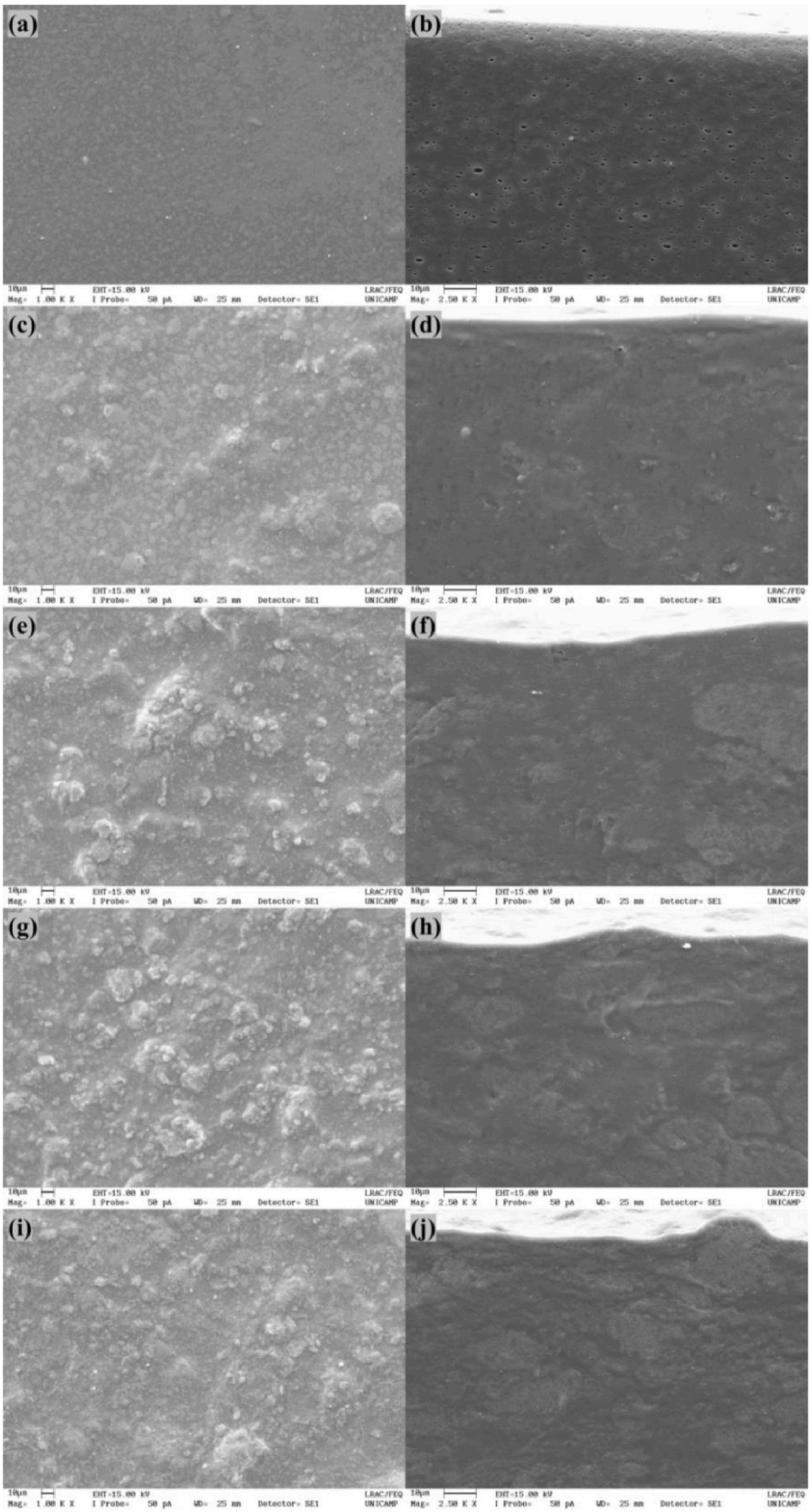


**Fig. 1.** Evaluation of the composite films morphology, in which (a), (c), (e), (g) and (i) refer to surface images with 1000 × magnification; and (b), (d), (f), (h) and (j) refer to the cross-sectional images, with 2500 × magnification. (a) and (b): SA/HC, (c) and (d): SA/HC/2%$SiO_2$, (e) and (f): SA/HC/6%$SiO_2$, (g) and (h): SA/HC/8% $SiO_2$, and (i) and (j): SA/HC/10%$SiO_2$.

agglomerated particles appear even in this concentration. With the gradual increase in the proportion of nano-$SiO_2$ added, surface and cross-section roughness increased, indicating poor dispersion and the formation of a composite material instead of a nanocomposite (Fig. 1 (e)–(j)). Despite the difficulty in obtaining a uniform morphology, these higher concentrations positively influenced the mechanical behavior, reported in the following topics of this work.

### 3.2. FT-IR analysis

Fig. 2(a) shows that all films scanned showed the typical functional groups of sodium alginate and hydrolyzed collagen. In the control film (SA/HC), the wavenumber of 3342 $cm^{-1}$ is associated to the –OH stretching. Characteristic C–H bending is noted at 2933 $cm^{-1}$ (Pereira et al., 2011). At the wavenumbers of 1598 and 1413 $cm^{-1}$ are the asymmetric and symmetric stretching vibrations of COO-, respectively (Santos et al., 2020), which are present in SA. The polypeptide backbone C–O stretching vibration of hydrolyzed collagen, and the formation of hydrogen bond between N–H stretch and C–O can also be found in the range of 1600–1700 $cm^{-1}$ (Riaz et al., 2018), causing overlapping of signals. The sharp peak registered at 1030 $cm^{-1}$ is assigned to the elongation of C–O groups (Pereira et al., 2011). The FT-IR spectra of the films remained unchanged despite the $SiO_2$ load, except for the 1088 $cm^{-1}$ peak, which is associated with the Si–O–Si bending vibrations (Mohammadi et al., 2019), that increased in intensity with the increment of $SiO_2$ percentages in the films. The low concentrations of nano-$SiO_2$ and the overlap of this characteristic bands with those of alginate justify the few changes to the spectrum (Júnior et al., 2021).

### 3.3. Thermogravimetric analysis (TGA)

Fig. 2 (c) and (d) show the TGA of sodium alginate-hydrolyzed collagen films added with nano-$SiO_2$. Note that the degradation behavior of all composite films occurred in two main distinct thermal events, which is typical for sodium alginate-based films (Fig. 2 (c)) (Aloui et al., 2021; Ho et al., 2020; Liu et al., 2017). Table 2 shows the initial degradation ($T_{onset}$) and maximum decomposition ($T_{max}$) temperatures for the mentioned thermal events. The first thermal event for all samples analyzed was registered around 80 °C, and corresponds to the evaporation of free water in the films.

The second thermal event is associated with the decomposition of the polymeric elements of the composites (Liu et al., 2017), the $T_{onset}$ and $T_{max}$ (second thermal event) of the control film were 217.51 and 230.07 °C, respectively (Table 2). These findings are very similar to those reported for pure sodium alginate films since hydrolyzed collagen thermal degradation occurs in a range close to that of sodium alginate (Aloui et al., 2021; Sadeghi and Hosseinzadeh, 2013). The addition of nano-$SiO_2$ on the sodium alginate-based films slightly increased their $T_{onset}$ and $T_{max}$ compared with the sodium alginate-hydrolyzed collagen control. This thermal behavior was especially noted for the second event of the SA/HC/10%$SiO_2$ film. Agreeing with the results presented in this work, the literature reports the general behavior of thermal stability

**Table 2**
Initial degradation ($T_{onset}$) and maximum decomposition ($T_{max}$) temperatures of SA/HC/$SiO_2$ composite films.

| Sample | First thermal event (°C) | | Second thermal event (°C) | |
|---|---|---|---|---|
| | $T_{onset}$ | $T_{max}$ | $T_{onset}$ | $T_{max}$ |
| **SA/HC** | 56.18 | 83.92 | 217.51 | 230.07 |
| **SA/HC/2%$SiO_2$** | 46.15 | 75.32 | 218.32 | 230.34 |
| **SA/HC/6%$SiO_2$** | 51.72 | 79.59 | 221.18 | 231.93 |
| **SA/HC/8%$SiO_2$** | 57.37 | 83.56 | 221.54 | 232.86 |
| **SA/HC/10%$SiO_2$** | 55.03 | 79.61 | 222.48 | 233.06 |

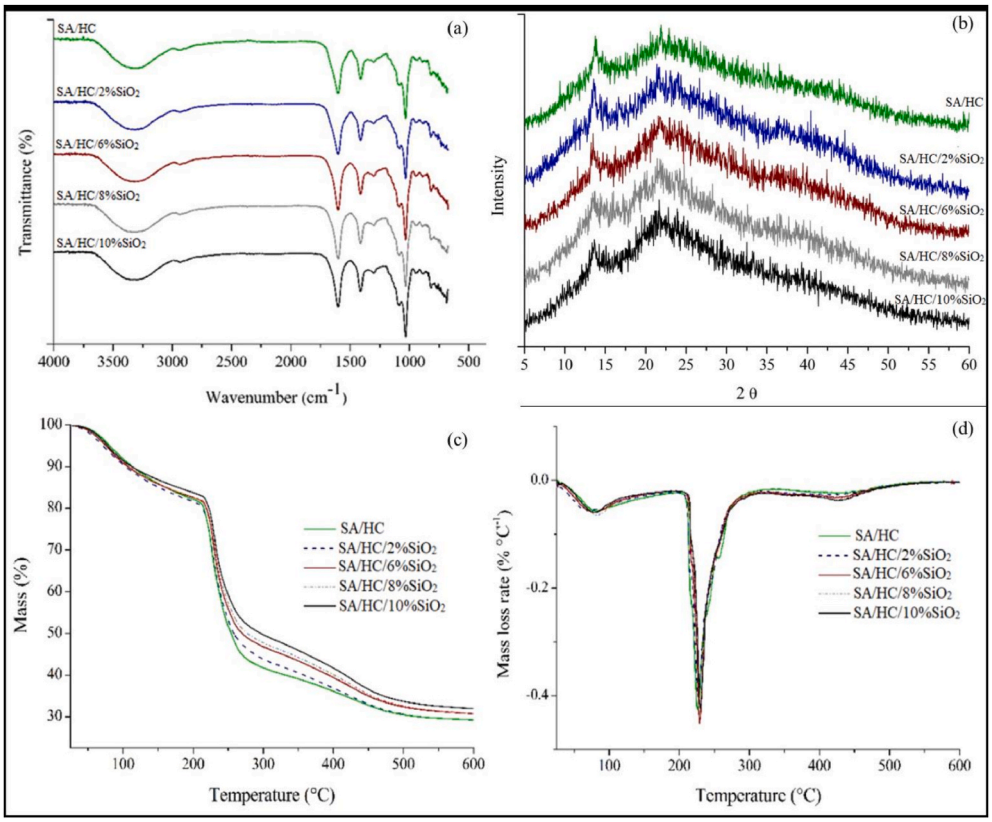


**Fig. 2.** FT-IR spectra (a), XRD pattern (b), TGA (c) and DTGA (d) of SA/HC/$SiO_2$ composite films.

enhancement of polymeric films due to $SiO_2$ incorporation. Zhu et al. reported a noticeable increase in the $T_{max}$ of starch-based extrusion--blown composite films incorporated with nano-$SiO_2$ (Zhu et al., 2021).

### 3.4. X-ray diffraction (XRD)

To investigate the crystallinity, Fig. 2 (b) shows the XRD spectra of the composite films based on sodium alginate and hydrolyzed collagen produced in this study. The diffraction peaks at 2θ for the composite films reveal semi-crystalline structures, predominantly amorphous. The spectra of the control sodium alginate-hydrolyzed collagen film registered a small peak at $2\theta \approx 14^{\circ}$ and a broad diffraction peak at $2\theta \approx 22^{\circ}$, which indicates low crystallinity (Bhagyaraj and Krupa, 2020). All formulated composites showed a coinciding pattern. With the addition of nano-$SiO_2$, the intensity of the crystalline peaks of the sodium alginate-based composites increased slightly. However, although it is not possible to make an accurate comparison on the diffractogram, the XRD patterns are of similar height, appearing to be mostly unchanged. Our results are different from those of Yang et al., who verified the addition of nano-$SiO_2$ to pure alginate films increased the amorphization of the polymer (Yang et al., 2016).

### 3.5. Thickness and mechanical properties

Table 3 shows thickness and mechanical properties of the composite films. The control film (SA/HC) had the lowest thickness among all films (160.6 ± 40.2 μm). However, the incorporation of up to 8% of nano-$SiO_2$ in the SA/HC films did not significantly influence the thickness results. On the other hand, note that the thickness of the SA/HC/10%$SiO_2$ film increased significantly compared with the SA/HC control film, which is attributed to the higher concentration of solids in the polymer matrix.

The tensile tests of SA/HC/$SiO_2$ composite films were carried out to evaluate the influence of $SiO_2$ nanoparticles on the mechanical properties. The results of tensile strength (TS) and elongation at break (EB) of the SA/HC control film were 18.2 ± 3.1 MPa and 19.5 ± 5.3%, respectively (Table 3). The addition of nano-$SiO_2$ in the SA/HC films increased TS values. However, although TS increased in the SA/HC/2% $SiO_2$, SA/HC/6%$SiO_2$ and SA/HC/8%$SiO_2$ films, it was not significantly different from the control sample. Only the addition of 10% nano-$SiO_2$ significantly increased the TS of the film compared with the control. For all concentrations of nano-$SiO_2$, the EB presented significantly higher results compared with the film without nano-$SiO_2$. Finally, the incorporation of nano-$SiO_2$ did not significantly influence the modulus of elasticity (ME), that is, the material's stiffness remained unchanged.

The improvement in TS for SA/HC/10%$SiO_2$ may be related to the strong interactions (hydrogen bonds) formed by the hydroxyl groups of the nano-$SiO_2$ with the carboxylic groups of the film polymeric matrix (Voon et al., 2012), reinforcing the material at high filler concentrations. The nano-$SiO_2$ concentrations below 10% had no significant influence in the TS, which corroborates the possible plasticizing effect of nano-$SiO_2$, justifying the large increase in elongation at break (EB). The increase in EB with the increase in the concentration of nano-$SiO_2$ has been attributed to a possible plasticizing role of $SiO_2$ nanoparticles (Salarbashi et al., 2021). The dispersion of nano-$SiO_2$ through the molecular matrix influence the interactions between polysaccharide-protein chain, and consequently improves the flexibility of the film (Hou et al., 2019). Furthermore, the agglomeration of filler particles may also have influenced this result, since such nano-$SiO_2$ agglomerates may have acted as internal lubricants, reducing friction forces in the polymer matrix. These results are in agreement with those found for composite films of gelatin/k-carrageenan/$SiO_2$ (Tabatabaei et al., 2018), and agar/sodium alginate/$SiO_2$ (Hou et al., 2019).

## 4. Conclusions

This study investigated the effects of different nano-$SiO_2$ loads as fillers in films based on sodium alginate and hydrolyzed collagen. The results showed $SiO_2$ nanoparticles concentrations ranging from 2 to 10% can be easily incorporated into SA/HC blends by casting, with significant improvement in mechanical properties and thermal stability. Only the highest concentration of nano-$SiO_2$ (10%) evaluated significantly improved the tensile strength of the films, from 18.2 MPa (control sample) to 25.4 MPa. However, all investigated nano-$SiO_2$ proportions increased elongation at break, suggesting a plasticizing effect. The films were much more flexible and resistant with 10% nano-$SiO_2$. Thermal stability improved slightly with the addition of nano-$SiO_2$, with the second $T_{onset}$ increase from 217.51 °C (control) to 222.48 °C). Therefore, the use of this ratio could represent an easy and effective strategy for possible future applications of these materials as food packaging.

## CRediT authorship contribution statement

**Luís Marangoni Júnior:** Conceptualization, Data curation, Formal analysis, Funding acquisition, Investigation, Methodology, Project administration, Resources, Writing – original draft, Writing – review & editing. **Plínio Ribeiro Rodrigues:** Data curation, Investigation, Writing – original draft. **Renan Garcia da Silva:** Formal analysis, Investigation, Writing – review & editing. **Roniérik Pioli Vieira:** Conceptualization, Data curation, Formal analysis, Funding acquisition, Investigation, Methodology, Project administration, Resources, Supervision, Writing – original draft, Writing – review & editing. **Rosa Maria Vercelino Alves:** Formal analysis, Funding acquisition, Investigation, Supervision, Writing – review & editing.

## Declaration of competing interest

The authors declare that they have no known competing financial interests or personal relationships that could have appeared to influence the work reported in this paper.

**Table 3**
Thickness and mechanical properties of SA/HC/$SiO_2$ composite films.

| Sample | Thickness (μm) | Tensile Strength (MPa) | Elongation at Break (%) | Modulus of elasticity (MPa) |
|---|---|---|---|---|
| **SA/HC** | 160.6 ± 40.2$^{b}$ | 18.2 ± 3.1$^{b}$ | 19.5 ± 5.3$^{b}$ | 424.0 ± 150.1$^{a}$ |
| **SA/HC/2%$SiO_2$** | 178.9 ± 37.5$^{ab}$ | 22.4 ± 1.0$^{ab}$ | 35.3 ± 5.1$^{a}$ | 502.5 ± 134.4$^{a}$ |
| **SA/HC/6%$SiO_2$** | 161.5 ± 35.1$^{b}$ | 20.2 ± 2.9$^{ab}$ | 30.2 ± 3.8$^{a}$ | 469.8 ± 25.9$^{a}$ |
| **SA/HC/8%$SiO_2$** | 180.6 ± 36.2$^{ab}$ | 21.8 ± 2.7$^{ab}$ | 30.3 ± 4.1$^{a}$ | 557.0 ± 39.5$^{a}$ |
| **SA/HC/10%$SiO_2$** | 195.0 ± 42.9$^{a}$ | 25.4 ± 0.2$^{a}$ | 35.8 ± 5.1$^{a}$ | 453.8 ± 55.8$^{a}$ |

The results are expressed as mean ± standard deviation.
$^{a, b, c}$ The means, followed by the same letter, in the column, do not differ at the 95% confidence level ($p < 0.05$).

## Acknowledgments

The authors acknowledge the National Council for Scientific and Technological Development (CNPq). This study was partly financed by the Coordination for the Improvement of Higher Education Personnel – Brazil (CAPES) – Financial Code 001. The authors thank *Espaço da Escrita – Pró-Reitoria de Pesquisa – UNICAMP* – for the language services provided.

## References

Abou-Okeil, A., Fahmy, H.M., El-Bisi, M.K., Ahmed-Farid, O.A., 2018. Hyaluronic acid/Na-alginate films as topical bioactive wound dressings. Eur. Polym. J. 109, 101–109. https://doi.org/10.1016/j.eurpolymj.2018.09.003.

Aloui, H., Deshmukh, A.R., Khomlaem, C., Kim, B.S., 2021. Novel composite films based on sodium alginate and gallnut extract with enhanced antioxidant, antimicrobial, barrier and mechanical properties. December 2020 Food Hydrocolloids 113, 106508. https://doi.org/10.1016/j.foodhyd.2020.106508.

ASTM-D882, 2018. Standard Test Method for Tensile Properties of Thin Plastic Sheeting. West Conshohocken.

Bhagyaraj, S., Krupa, I., 2020. Alginate-mediated synthesis of hetero-shaped silver nanoparticles and their hydrogen peroxide sensing ability. Molecules 25 (3), 435. https://doi.org/10.3390/molecules25030435.

Castiello, D., Chiellini, E., Cinelli, P., D'Antone, S., Puccini, M., Salvadori, M., Seggiani, M., 2009. Polyethylene-collagen hydrolizate thermoplastic blends: thermal and mechanical properties. J. Appl. Polym. Sci. 114 (6), 3827–3834. https://doi.org/10.1002/app.31000.

Condés, M.C., Añón, M.C., Dufresne, A., Mauri, A.N., 2018. Composite and nanocomposite films based on amaranth biopolymers. Food Hydrocolloids 74, 159–167. https://doi.org/10.1016/j.foodhyd.2017.07.013.

Denis, A., Brambati, N., Dessauvages, B., Guedj, S., Ridoux, C., Meffre, N., Autier, C., 2008. Molecular weight determination of hydrolyzed collagens. Food Hydrocolloids 22 (6), 989–994. https://doi.org/10.1016/j.foodhyd.2007.05.016.

Gheorghita Puscaselu, R., Lobiuc, A., Dimian, M., Covasa, M., 2020. Alginate: from food industry to biomedical applications and management of metabolic disorders. Polymers. https://doi.org/10.3390/polym12102417.

Guha, I.F., 2010. Effects of Silica Nanoparticle Surface Treatment and Average Diameter on the Physical and Mechanical Properties of Poly(dimethylsiloxane)-Silica Nanocomposites. Massachussetts Institute of Technology.

Ho, T.C., Kim, M.H., Cho, Y.-J., Park, J.-S., Nam, S.Y., Chun, B.-S., 2020. Gelatin-sodium alginate based films with Pseuderanthemum palatiferum (Nees) Radlk. freeze-dried powder obtained by subcritical water extraction. Food Packaging and Shelf Life 24, 100469. https://doi.org/10.1016/j.fpsl.2020.100469.

Hou, X., Xue, Z., Xia, Y., Qin, Y., Zhang, G., Liu, H., Li, K., 2019. Effect of SiO2 nanoparticle on the physical and chemical properties of eco-friendly agar/sodium alginate nanocomposite film. Int. J. Biol. Macromol. 125, 1289–1298. https://doi.org/10.1016/j.ijbiomac.2018.09.109.

ISO-4593, 1993. Plastics: Film and Sheeting Determination of Thickness by Mechanical Scanning (Switzerland).

Júnior, L.M., da Silva, R.G., Anjos, C.A.R., Vieira, R.P., Alves, R.M.V., 2021. Effect of low concentrations of SiO2 nanoparticles on the physical and chemical properties of sodium alginate-based films. Carbohydr. Polym. 118286. https://doi.org/10.1016/j.carbpol.2021.118286.

Kloster, G.A., Muraca, D., Mosiewicki, M.A., Marcovich, N.E., 2017. Magnetic composite films based on alginate and nano-iron oxide particles obtained by synthesis "in situ. Eur. Polym. J. 94, 43–55. https://doi.org/10.1016/j.eurpolymj.2017.06.041.

Liu, S., Li, Y., Li, L., 2017. Enhanced stability and mechanical strength of sodium alginate composite films. Carbohydr. Polym. 160, 62–70. https://doi.org/10.1016/j.carbpol.2016.12.048.

Marangoni Júnior, L., Rodrigues, P.R., da Silva, R.G., Vieira, R.P., Alves, R.M.V., 2021a. Sustainable packaging films composed of sodium alginate and hydrolyzed collagen: preparation and characterization. Food Bioprocess Technol. 14 (12), 2336–2346. https://doi.org/10.1007/s11947-021-02727-7.

Marangoni Júnior, L., Silva, R. G. da, Vieira, R.P., Alves, R.M.V., 2021b. Water vapor sorption and permeability of sustainable alginate/collagen/SiO2 composite films. LWT (Lebensm.-Wiss. & Technol.) 152, 112261. https://doi.org/10.1016/j.lwt.2021.112261.

Marangoni, L., Fávaro Perez, M.Â., Torres, C.D., Cristianini, M., Massaharu Kiyataka, P. H., Albino, A.C., Rodrigues Anjos, C.A., 2020. Effect of high-pressure processing on the migration of ε-caprolactam from multilayer polyamide packaging in contact with food simulants. Food Packaging and Shelf Life 26. https://doi.org/10.1016/j.fpsl.2020.100576.

Mohammadi, M., Khorrami, M.K., Ghasemzadeh, H., 2019. ATR-FTIR spectroscopy and chemometric techniques for determination of polymer solution viscosity in the presence of SiO2 nanoparticle and salinity. Spectrochim. Acta Mol. Biomol. Spectrosc. 220, 117049. https://doi.org/10.1016/j.saa.2019.04.041.

Moreira Gonçalves, S., Gomes Motta, J.F., Ribeiro-Santos, R., Hidalgo Chávez, D.W., Ramos de Melo, N., 2020. Functional and antimicrobial properties of cellulose acetate films incorporated with sweet fennel essential oil and plasticizers. Curr. Res. Food Sci. 3, 1–8. https://doi.org/10.1016/j.crfs.2020.01.001.

Mousavi, S.N., Daneshvar, H., Seyed Dorraji, M.S., Ghasempour, Z., Panahi-Azar, V., Ehsani, A., 2021. Starch/alginate/Cu-g-C3N4 nanocomposite film for food packaging. Mater. Chem. Phys. 267, 124583. https://doi.org/10.1016/j.matchemphys.2021.124583.

Nesic, A., Castillo, C., Castaño, P., Cabrera-Barjas, G., Serrano, J., C. M. B. T.-B. P., 2020. Chapter 8 - bio-based packaging materials. In: Galanakis, I. (Ed.). Elsevier, pp. 279–309. https://doi.org/10.1016/B978-0-12-818493-6.00008-7.

Pei, Y., Yang, J., Liu, P., Xu, M., Zhang, X., Zhang, L., 2013. Fabrication, properties and bioapplications of cellulose/collagen hydrolysate composite films. Carbohydr. Polym. 92 (2), 1752–1760. https://doi.org/10.1016/j.carbpol.2012.11.029.

Pereira, R., Tojeira, A., Vaz, D.C., Mendes, A., Bártolo, P., 2011. Preparation and characterization of films based on alginate and aloe vera. Int. J. Polym. Anal. Char. 16 (7), 449–464. https://doi.org/10.1080/1023666X.2011.599923.

Riaz, T., Zeeshan, R., Zarif, F., Ilyas, K., Muhammad, N., Safi, S.Z., Rehman, I.U., 2018. FTIR analysis of natural and synthetic collagen. Appl. Spectrosc. Rev. 53 (9), 703–746. https://doi.org/10.1080/05704928.2018.1426595.

Sadeghi, M., Hosseinzadeh, H., 2013. Synthesis and properties of collagen-g-poly(sodium acrylate-co-2-hydroxyethylacrylate) superabsorbent hydrogels. Braz. J. Chem. Eng. 30 (2), 379–389. https://doi.org/10.1590/S0104-66322013000200015.

Salarbashi, D., Tafaghodi, M., Bazzaz, B.S.F., Mohammad Aboutorabzade, S., Fathi, M., 2021. pH-sensitive soluble soybean polysaccharide/SiO2 incorporated with curcumin for intelligent packaging applications. Food Sci. Nutr. 9 (4), 2169–2179. https://doi.org/10.1002/fsn3.2187.

Santos, N.L., Ragazzo, G. de O., Cerri, B.C., Soares, M.R., Kieckbusch, T.G., da Silva, M. A., 2020. Physicochemical properties of konjac glucomannan/alginate films enriched with sugarcane vinasse intended for mulching applications. Int. J. Biol. Macromol. 165, 1717–1726. https://doi.org/10.1016/j.ijbiomac.2020.10.049.

Seggiani, M., Gigante, V., Cinelli, P., Coltelli, M.-B., Sandroni, M., Anguillesi, I., Lazzeri, A., 2019. Processing and mechanical performances of Poly(Butylene Succinate–co–Adipate) (PBSA) and raw hydrolyzed collagen (HC) thermoplastic blends. Polym. Test. 77, 105900. https://doi.org/10.1016/j.polymertesting.2019.105900.

Tabatabaei, R.H., Jafari, S.M., Mirzaei, H., Nafchi, A.M., Dehnad, D., 2018. Preparation and characterization of nano-SiO2 reinforced gelatin-k-carrageenan biocomposites. Int. J. Biol. Macromol. 111, 1091–1099. https://doi.org/10.1016/j.ijbiomac.2018.01.116.

Tian, S., Gao, W., Liu, Y., Kang, W., Yang, H., 2020. Effects of surface modification Nano-SiO2 and its combination with surfactant on interfacial tension and emulsion stability. Colloids Surf. A Physicochem. Eng. Asp. 595, 124682. https://doi.org/10.1016/j.colsurfa.2020.124682.

Vianna, T.C., Marinho, C.O., Júnior, L.M., Ibrahim, S.A., Vieira, R.P., 2021. Essential oils as additives in active starch-based food packaging films: a review. Int. J. Biol. Macromol. https://doi.org/10.1016/j.ijbiomac.2021.05.170.

Voon, H.C., Bhat, R., Easa, A.M., Liong, M.T., Karim, A.A., 2012. Effect of addition of halloysite nanoclay and SiO 2 nanoparticles on barrier and mechanical properties of bovine gelatin films. Food Bioprocess Technol. 5 (5), 1766–1774. https://doi.org/10.1007/s11947-010-0461-y.

Yang, M., Xia, Y., Wang, Y., Zhao, X., Xue, Z., Quan, F., Zhao, Z., 2016. Preparation and property investigation of crosslinked alginate/silicon dioxide nanocomposite films. J. Appl. Polym. Sci. 133 (22), 1–9. https://doi.org/10.1002/app.43489.

Zhang, G., Sun, A., Li, W., Liu, T., Su, Z., 2006. Mass spectrometric analysis of enzymatic digestion of denatured collagen for identification of collagen type. J. Chromatogr. A 1114 (2), 274–277. https://doi.org/10.1016/j.chroma.2006.03.039.

Zhang, Z.-H., Xu, J.-Y., Yang, X.-L., 2021. MXene/sodium alginate gel beads for adsorption of methylene blue. Mater. Chem. Phys. 260, 124123. https://doi.org/10.1016/j.matchemphys.2020.124123.

Zhu, J., Gao, W., Wang, B., Kang, X., Liu, P., Cui, B., Abd El-Aty, A.M., 2021. Preparation and evaluation of starch-based extrusion-blown nanocomposite films incorporated with nano-ZnO and nano-SiO2. Int. J. Biol. Macromol. 183, 1371–1378. https://doi.org/10.1016/j.ijbiomac.2021.05.118.